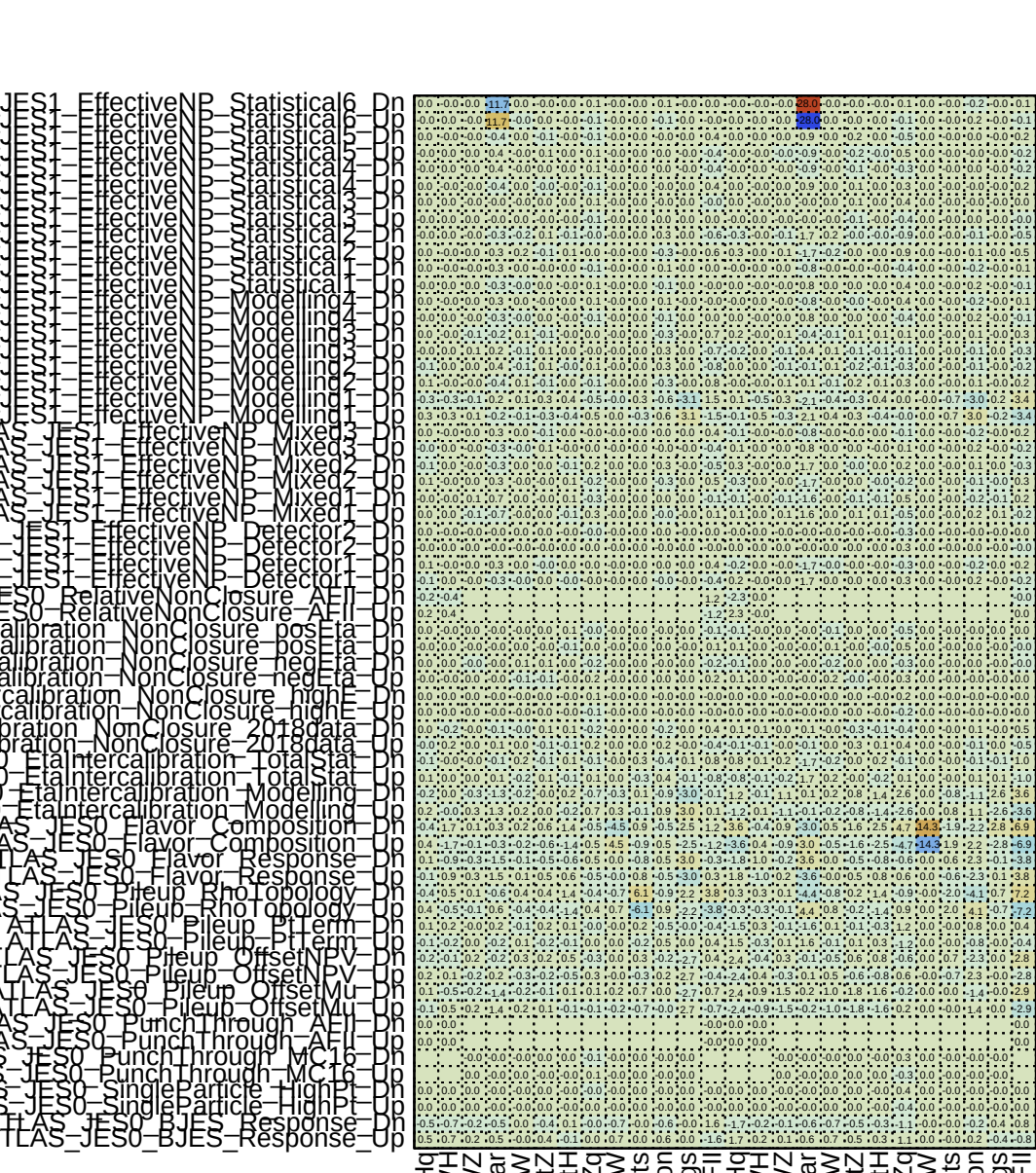
JES1_EffectiveNP_Statistical6_Dn
JES1_EffectiveNP_Statistical6_Up
JES1_EffectiveNP_Statistical5_Dn
JES1_EffectiveNP_Statistical5_Up
JES1_EffectiveNP_Statistical4_Dn
JES1_EffectiveNP_Statistical4_Up
JES1_EffectiveNP_Statistical3_Dn
JES1_EffectiveNP_Statistical3_Up
JES1_EffectiveNP_Statistical2_Dn
JES1_EffectiveNP_Statistical2_Up
JES1_EffectiveNP_Statistical1_Dn
JES1_EffectiveNP_Statistical1_Up
JES1_EffectiveNP_Modelling4_Dn
JES1_EffectiveNP_Modelling4_Up
JES1_EffectiveNP_Modelling3_Dn
JES1_EffectiveNP_Modelling3_Up
JES1_EffectiveNP_Modelling2_Dn
JES1_EffectiveNP_Modelling2_Up
JES1_EffectiveNP_Modelling1_Dn
JES1_EffectiveNP_Modelling1_Up
AS_JES1_EffectiveNP_Mixed3_Dn
AS_JES1_EffectiveNP_Mixed3_Up
AS_JES1_EffectiveNP_Mixed2_Dn
AS_JES1_EffectiveNP_Mixed2_Up
AS_JES1_EffectiveNP_Mixed1_Dn
AS_JES1_EffectiveNP_Mixed1_Up
_JES1_EffectiveNP_Detector2_Dn
_JES1_EffectiveNP_Detector2_Up
_JES1_EffectiveNP_Detector1_Dn
_JES1_EffectiveNP_Detector1_Up
ES0_RelativeNonClosure_AFII_Dn
ES0_RelativeNonClosure_AFII_Up
alibration_NonClosure_posEta_Dn
alibration_NonClosure_posEta_Up
alibration_NonClosure_negEta_Dn
alibration_NonClosure_negEta_Up
calibration_NonClosure_highE_Dn
calibration_NonClosure_highE_Up
bration_NonClosure_2018data_Dn
bration_NonClosure_2018data_Up
0_EtaIntercalibration_TotalStat_Dn
0_EtaIntercalibration_TotalStat_Up
_EtaIntercalibration_Modelling_Dn
_EtaIntercalibration_Modelling_Up
AS_JES0_Flavor_Composition_Dn
AS_JES0_Flavor_Composition_Up
LAS_JES0_Flavor_Response_Dn
LAS_JES0_Flavor_Response_Up
S_JES0_Pileup_RhoTopology_Dn
S_JES0_Pileup_RhoTopology_Up
ATLAS_JES0_Pileup_PtTerm_Dn
ATLAS_JES0_Pileup_PtTerm_Up
LAS_JES0_Pileup_OffsetNPV_Dn
LAS_JES0_Pileup_OffsetNPV_Up
TLAS_JES0_Pileup_OffsetMu_Dn
TLAS_JES0_Pileup_OffsetMu_Up
AS_JES0_PunchThrough_AFII_Dn
AS_JES0_PunchThrough_AFII_Up
S_JES0_PunchThrough_MC16_Dn
S_JES0_PunchThrough_MC16_Up
S_JES0_SingleParticle_HighPt_Dn
S_JES0_SingleParticle_HighPt_Up
TLAS_JES0_BJES_Response_Dn
TLAS_JES0_BJES_Response_Up
SR_BDT_tHq_2L1TAU_SS_tHq
SR_BDT_tHq_2L1TAU_SS_tWH
SR_BDT_tHq_2L1TAU_SS_tWZ
SR_BDT_tHq_2L1TAU_SS_ttbar
SR_BDT_tHq_2L1TAU_SS_ttW
SR_BDT_tHq_2L1TAU_SS_ttZ
SR_BDT_tHq_2L1TAU_SS_ttH
SR_BDT_tHq_2L1TAU_SS_tZq
SR_BDT_tHq_2L1TAU_SS_singletop_tW
SR_BDT_tHq_2L1TAU_SS_Zjets
SR_BDT_tHq_2L1TAU_SS_Diboson
SR_BDT_tHq_2L1TAU_SS_minor_bkgs
SR_BDT_tHq_2L1TAU_SS_minor_bkgs_AFII
CR_Bkg_2L1TAU_SS_tHq
CR_Bkg_2L1TAU_SS_tWH
CR_Bkg_2L1TAU_SS_tWZ
CR_Bkg_2L1TAU_SS_ttbar
CR_Bkg_2L1TAU_SS_ttW
CR_Bkg_2L1TAU_SS_ttZ
CR_Bkg_2L1TAU_SS_ttH
CR_Bkg_2L1TAU_SS_tZq
CR_Bkg_2L1TAU_SS_singletop_tW
CR_Bkg_2L1TAU_SS_Zjets
CR_Bkg_2L1TAU_SS_Diboson
CR_Bkg_2L1TAU_SS_minor_bkgs
CR_Bkg_2L1TAU_SS_minor_bkgs_AFII